Factors Controlling Activity and Selectivity for SCR of NO by Hydrogen over Supported Platinum Catalysts

Junji Shibata, Masanori Hashimoto, Ken-ichi Shimizu, Hisao Yoshida, Tadashi Hattori, and Atsushi Satsuma*

Department of Applied Chemistry, Graduate School of Engineering, Nagoya University, Chikusa-ku, Nagoya 464-8603, Japan

Received: July 24, 2004; In Final Form: September 8, 2004

The selective catalytic reduction of NO by H_2 (H_2-SCR) was carried out with Pt catalysts supported on various zeolites and nonzeolitic metal oxides. NO conversion and N_2 selectivity were strongly dependent on the supports; a high NO conversion was obtained over Pt/SiO_2-Al_2O_3 and Pt/SiO_2, while the N_2 selectivity was high on Pt/zeolites, particularly Pt/MFI. The strong effect of supports on the activity and selectivity for the H_2-SCR was discussed based on Pt dispersion measured by the CO−H_2 titration, the oxidation state of Pt estimated with Pt L_{III}-edge XAFS, and the acid properties of the supports. It was clarified that the SCR activity was controlled by the oxidation state of Pt (i.e., the less oxidized Pt showed the higher turnover frequency for the H_2-SCR). On the other hand, the N_2 selectivity was related to the acid strength of the supports. The formation of the NH_4^+ ion under the H_2-SCR reaction was observed by in situ IR spectra, and the surface NH_4^+ concentration was higher on the more acidic supports. The transient reaction tests revealed that the NH_4^+ ion reacts with NO + O_2 to produce N_2. A bifunctional mechanism was proposed, which includes the NH_3 formation through NO reduction by H_2 on a Pt surface, followed by storage of NH_4^+ on the Brønsted acid site of acidic supports, and the selective N_2 formation by the well-established NH_3-SCR mechanism on the acid sites of the supports.

1. Introduction

The selective catalytic reduction of NO by hydrocarbons (HC-SCR) has received much attention because of its potential application for the removal of NO_x from exhausts containing excess oxygen. Since the pioneering studies by Iwamoto et al.[1] and Held et al.,[2] extensive research has been done on the development of various types of de-NO_x catalysts. The supported Pt catalyst is known to be the most active precious metal catalyst at low temperatures and has a high durability against sulfur and water vapor.[3,4] However, the formation of N_2O as a byproduct, which is a powerful greenhouse gas, is a serious problem of the Pt-based catalysts for use in HC-SCR.[5−7] Although HC-SCR on Pt catalysts was attempted to suppress N_2O production by using various supports[8] and additives,[9,10] changing platinum precursors[11] and preparing a sol−gel method,[12] no drastic improvement in the selectivity of HC-SCR was achieved. Since the HC-SCR performance may come from a complicated reaction mechanism,[4,8,13−15] it is difficult to distinguish the involvements of Pt and the supports in the HC-SCR performance.

Recently, the selective reduction of NO by hydrogen (H_2-SCR) on supported Pt catalysts has been paid much attention because of the high activity at low temperatures around 373 K.[16−27] The reaction mechanism of the H_2-SCR should be simpler than that of HC-SCR since H_2 is unlikely to be activated on metal oxide supports at temperatures lower than 373 K. For the H_2-SCR, the activity and the selectivity into N_2 are strongly affected by the supports and additives.[17,19−22] For example, the use of mixed oxide supports[12] and perovskite-type supports[19−21] including transition metal elements was reported to be effective for the suppression of the N_2O production. In our previous communication, the strong effect of the supports was also observed in the H_2-SCR over supported Pt catalysts (i.e., the high N_2 selectivity was obtained using acidic supports, such as zeolites).[23] Although effective catalysts for the suppression of the N_2O formation have been proposed, the role and the desirable characteristic of Pt and the supports are not well-clarified.

In the present study, the H_2-SCR performance under excess oxygen was examined using a series of Pt catalysts supported on various materials. Through characterizations of the Pt species and surface adspecies under the H_2-SCR, the controlling factors for the activity and the N_2 selectivity on the H_2-SCR over supported Pt catalysts are discussed on the basis of the involvements of Pt and the support materials and the reaction pathways on these surfaces.

2. Experimental Procedures

Table 1 shows the supported Pt catalysts employed in the present study. H-BEA, H-Y, SiO_2-Al_2O_3, SiO_2, Al_2O_3, and MgO were supplied by the Committee of Reference Catalysts, Catalysis Society of Japan (JRC-HB25, JRC-Z-HY4.8, JRC-SAL-2, JRC-SIO-8, JRC-ALO-4, and JRC-MGO-4 100A).[28,29] H-MOR (Si/Al = 7.7) and H-MFI (Si/Al = 20) were supplied by the Tosoh Corporation. Pt/zeolite catalysts were prepared by a conventional ion-exchange in an aqueous $Pt(NH_3)_4Cl_2$ solution at room temperature. After filtration, the sample was washed with distilled water and dried at 393 K. Nonzeolitic metal oxide supported Pt catalysts were prepared by impregnating an aqueous $Pt(NH_3)_4Cl_2$ solution. These precursors were

* To whom correspondence should be addressed. Fax: +81-52-789-3193. E-mail: satsuma@apchem.nagoya-u.ac.jp.

10.1021/jp046705v CCC: $27.50
Published on Web 10/26/2004

TABLE 1: List of Pt Catalysts

catalysts	preparation method	support	Pt content/ wt %	Pt dispersion before reaction/ %[a]
Pt/MOR	ion exchange	H-MOR (Si/Al = 7.7)[b]	1.0	37
Pt/MFI	ion exchange	H-MFI (Si/Al = 20)[b]	0.8	31
Pt/BEA	ion exchange	JRC-HB25 (Si/Al = 13)[c]	1.3	16
Pt/Y	ion exchange	JRC-Z-HY4.8 (Si/Al = 2.4)[c]	1.6	6
Pt/SiO_2-Al_2O_3	impregnation	JRC-SAL-2 (Si/Al = 5.3)[c]	1.0	13
Pt/SiO_2	impregnation	JRC-SIO-8[c]	1.0	6
Pt/Al_2O_3-22[d]	impregnation	JRC-ALO-4[c]	1.0	22
Pt/Al_2O_3-35[e]	impregnation	JRC-ALO-4[c]	1.0	35
Pt/Al_2O_3-60	impregnation	JRC-ALO-4[c]	1.0	60
Pt/MgO	impregnation	JRC-MGO-4 100A[c]	1.0	37

[a] Estimated from CO−H_2 titration.[30] [b] Supplied by Tosoh Corporation. [c] Supplied by the Committee of Reference Catalysts, Catalysis Society of Japan. [d] Orepared by treatment of Pt/Al_2O_3-60 in flowing H_2 at 823 K for 24 h. [e] Prepared by treatment of Pt/Al_2O_3-60 in flowing H_2 at 823 K for 48 h.

calcined at 773 K for 3 h in flowing dried air. Pt/Al_2O_3-22 and -35 with a low Pt dispersion were prepared through calcination of Pt/Al_2O_3-60 in flowing H_2 at 823 K for 24 and 48 h, respectively. The Pt content in the Pt/zeolites was analyzed by inductively coupled plasma emission spectroscopy (ICP, Jarrel-Ash MODEL 975). The Pt content was about 1 wt % for all the catalysts. The dispersion of the Pt catalysts before and after the H_2-SCR was measured using the CO−H_2 titration method developed by Komai et al.[30]

The catalytic test was performed using a fixed-bed flow reactor by passing a mixture of 1000 ppm NO, 5000 ppm H_2, and 6.7% O_2 in He at the rate of 100 cm^3 min^{-1} over a 0.05 g catalyst (W/F = 0.030 g cm^{-3} s, GHSV = 78 000 h^{-1}). Prior to the experiment, the catalyst was heated in 6.7% O_2/He at 773 K for 1 h. After reaching a steady state, the effluent gas was analyzed by a gas chromatograph equipped with a Porapak Q column (2 m) for separation of N_2O and a MS 13X column (6 m) for separation of N_2, H_2, and O_2. NO and NO_2 (NO_x) were analyzed by a chemiluminescence NO_x analyzer (Best BCL-100uH). The main products were N_2, N_2O, and H_2O. NH_3 was not detected in the gas phase on all the Pt catalysts. The reaction results were described in terms of the NO_x conversion, H_2 conversion, and N_2 selectivity. The N_2 selectivity was determined as (N_2 yield)/(N_2 yield + N_2O yield) × 100 (%).

The Pt L_{III}-edge XAFS spectra of the catalysts after the H_2-SCR were recorded at the BL-10B station[31] at KEK-PF with a Si(311) channel cut monochromator in the transmission mode at room temperature. The catalysts after the H_2-SCR were cooled to room temperature in flowing He, exposed to ambient atmosphere, and then packed in the cell. The incident and transmitted X-rays were monitored by ionization chambers filled with Ar/N_2 (Ar/N_2 = 15/85) and Ar/N_2 (Ar/N_2 = 50/50) gases, with the length of 17 and 31 cm, respectively. The sample thickness was regulated for the total X-ray absorbance to be less than 4. Such a choice of detection gases and adjustment of the appropriate sample thickness made the effect of higher harmonics negligible.

The in situ IR spectra were recorded using a JASCO FT/IR-620 equipped with a quartz IR cell connected to a conventional flow reaction system, which was used in our previous studies.[32,33] The sample was pressed into a 0.05 g self-supporting wafer and mounted into a quartz IR cell with CaF_2 windows. The spectra were measured by accumulating 20 scans at a resolution of 2 cm^{-1}. A reference spectrum of the catalyst wafer in flowing He was taken at 348 K and was subtracted from each spectrum under the reaction conditions. Prior to each experiment, the catalyst disk was heated in 6.7% O_2/He at 773 K for 1 h, followed by cooling to 348 K and purging for 30 min in He. A flow of various gas mixtures was then fed at a rate of 100 cm^3 min^{-1} at 348 K. The composition of the reaction mixtures was the same as in the corresponding catalytic tests.

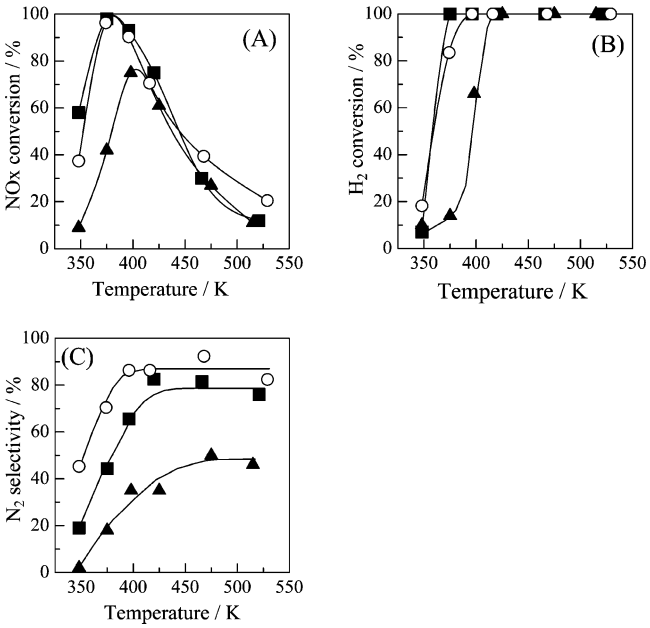

Figure 1. (A) NO_x conversion, (B) H_2 conversion, and (C) N_2 selectivity over (○) Pt/ MFI, (■) Pt/SiO_2-Al_2O_3, and (▲) Pt/MgO. Conditions: [NO] = 1000 ppm, [H_2] = 5000 ppm, [O_2] = 6.7%, and GHSV = 78 000 h^{-1}.

3. Results

3.1. H_2-SCR over Various Pt Catalysts. Figure 1 shows the NO_x conversion, H_2 conversion, and N_2 selectivity over Pt/MFI, Pt/SiO_2-Al_2O_3, and Pt/MgO as a function of the reaction temperatures. For all the catalysts, the NO_x conversion increased with the reaction temperature, reached a maximum at 373−423 K, and then decreased without any further increase in the temperature. The H_2 conversion on each catalyst reached 100% at the temperatures where the maximum NO conversion was observed. The NO and H_2 conversions on Pt/MFI and Pt/SiO_2-Al_2O_3 were higher than that on Pt/MgO below 398 K. The N_2 selectivity increased as the reaction temperature increased. For example, the N_2 selectivity on Pt/MFI was 45% at 348 K and reached 82% at 398 K where the H_2 conversion was 100%. In the temperature range from 398 to 523 K, the N_2 selectivity on Pt/MFI was 82−92%, which is as high as that on $Pt/La_{0.5}Ce_{0.5}$-MnO_3 and $Pt/La_{0.7}Sr_{0.2}Ce_{0.1}FeO_3$.[19,20] The N_2 selectivity was in the order of Pt/MFI > Pt/SiO_2-Al_2O_3 > Pt/MgO for the whole range of temperatures.

TABLE 2: NO_x Conversion and N_2 Selectivity for SCR of NO by H_2 at 348 K

catalysts	NO_x conversion/ %	N_2 yield/ %	N_2O yield/ %	N_2 selectivity/ %	TOF/ s^{-1}
Pt/MOR[a]	32	9	23	29	0.088
Pt/MFI	37	17	20	45	0.094
Pt/BEA	30	12	18	40	0.036
Pt/Y	20	6	14	31	0.047
Pt/SiO_2-Al_2O_3	58	11	47	19	0.122
Pt/SiO_2	44	4	40	8	0.249
Pt/Al_2O_3-22	24	1	23	6	0.058
Pt/Al_2O_3-35	26	3	23	11	0.019
Pt/Al_2O_3-60	19	2	17	9	0.010
Pt/MgO	9	0.2	9	2	0.007

[a] W/F = 0.024 g cm^{-3} s.

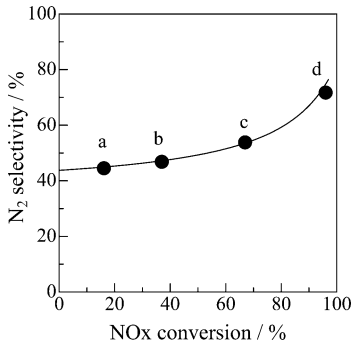

Figure 2. N_2 selectivity as a function of NO_x conversion over Pt/MFI at 373 K. NO_x conversion was adjusted by varying W/F at (a) 0.0035, (b) 0.0074, (c) 0.015, and (d) 0.030 g cm^3 s^{-1}, respectively.

Table 2 shows the NO_x conversion and N_2 selectivity of various catalysts at 348 K at W/F = 0.030 g cm^{-3} s. Only in the case of Pt/MOR, the data were taken at W/F = 0.024 g cm^{-3} s. At these reaction conditions, both the conversions of NO and H_2 were less than 60% for all the catalysts. The NO_x conversion and N_2 selectivity were significantly affected by the supports. A high NO_x conversion was obtained over Pt/ SiO_2-Al_2O_3 (58%) and Pt/SiO_2 (44%), while the NO_x conversion on Pt/MgO (9%) was the lowest. The NO_x conversion on Pt/Al_2O_3 was slightly affected by the Pt dispersion. The N_2 selectivity was relatively high on the Pt/zeolites and was the highest on Pt/MFI. The order of the N_2 selectivity among the Pt/zeolites was Pt/MFI > Pt/BEA > Pt/Y, Pt/MOR. Among the Pt catalysts on the nonzeolitic metal oxide supports (abbreviated as Pt/metal-oxides), Pt/SiO_2-Al_2O_3 exhibited the highest N_2 selectivity (19%). The N_2 selectivity on Pt/Al_2O_3 was low irrespective of the Pt dispersion.

To investigate the influence of the NO_x conversion on the N_2 selectivity, the H_2-SCR on Pt/MFI was carried out at various W/F values ranging from 0.004 to 0.03 g cm^{-3} s at 373 K. Figure 2 shows the dependence of the N_2 selectivity on the NO conversion. A line can be extrapolated to 44% when the NO_x conversion is 0%, indicating there are parallel reaction pathways to form N_2 and N_2O. The change in the N_2 selectivity is only within 7% when the NO_x conversion is below 60%. The contribution of the successive reaction of N_2O to N_2 is small, and these products mainly form through a parallel reaction pathway in this NO_x conversion range. On the other hand, the N_2 selectivity gradually increased when the NO_x conversion exceeded 60%, indicating the presence of the successive reduction of N_2O at a higher NO_x conversion.

3.2. CO-H_2 Titration. Table 3 shows the Pt dispersion measured by the CO-H_2 titration on various Pt catalysts after a series of the H_2-SCR reactions from 523 to 348 K. For the supported Pt catalysts except for Pt/BEA, Pt/Y, and Pt/Al_2O_3-35, the Pt dispersion decreased after the H_2-SCR, which indicates that the Pt species was agglomerated under the H_2-SCR. The Pt dispersion was high (29−42%) for Pt/MgO, Pt/Al_2O_3-35, and Pt/Al_2O_3-60, while it was below 16% for the other Pt catalysts.

TABLE 3: Properties of Pt on Supported Pt Catalysts

catalysts	Pt dispersion before reaction/%[a]	Pt dispersion after reaction/%[a]	integrated white line intensity after reaction[b]
Pt/MOR	37	12	4.21
Pt/MFI	31	14	4.14
Pt/BEA	16	16	5.01
Pt/Y	6	6	5.03
Pt/SiO_2-Al_2O_3	13	10	4.16
Pt/SiO_2	6	4	3.97
Pt/Al_2O_3-22	22	13	5.06
Pt/Al_2O_3-35	35	38	5.88
Pt/Al_2O_3-60	60	42	7.11
Pt/MgO	37	29	7.87

[a] Estimated from CO−H_2 titration.[30] [b] Pt foil: 3.80; PtO_2: 7.29.

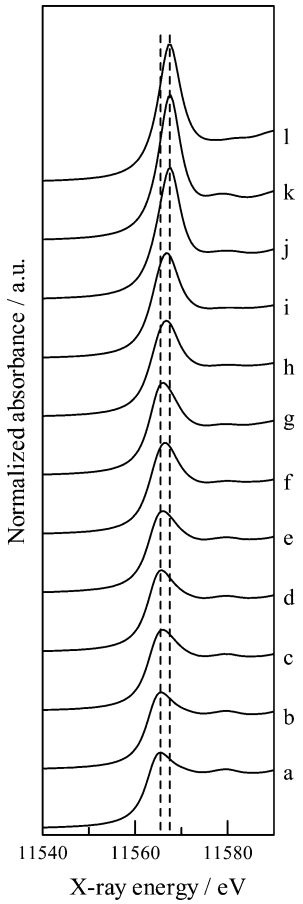

Figure 3. Pt L_{III}-edge XANES spectra of (a) Pt foil, (b) Pt/SiO_2, (c) Pt/MFI, (d) Pt/ SiO_2-Al_2O_3, (e) Pt/MOR, (f) Pt/BEA, (g) Pt/Y, (h) Pt/Al_2O_3-22, (i) Pt/Al_2O_3-35, (j) Pt/Al_2O_3-60, (k) Pt/MgO, and (l) PtO_2. The spectra of the catalysts (b−k) were measured after the H_2-SCR reaction.

3.3. Pt L_{III}-Edge XAFS. Figure 3 shows the Pt L_{III}-edge XANES of supported Pt catalysts after the H_2-SCR. The positions of the white line in these XANES spectra were different from catalyst to catalyst. For Pt/SiO_2, Pt/MFI, Pt/SiO_2-Al_2O_3, and Pt/MOR, the XANES spectra had a white line at 11566 eV and were similar to a spectrum of Pt foil. On the other hand, the XANES spectra of Pt/Al_2O_3-60 and Pt/MgO had a white line at 11568 eV and were similar to the spectrum

of PtO_2. For Pt/BEA, Pt/Y, Pt/Al_2O_3-22, and Pt/Al_2O_3-35, a white line was observed between 11566 and 11568 eV, which indicates that these catalysts contain both metallic Pt and oxidized Pt species such as PtO and PtO_2.

It is well-established that the white line intensity at the Pt L_{III}-edge is an informative indication for the oxidation state of platinum since the white line of the Pt L_{III}-edge XANES spectrum is assigned to the electron transition from the $2p_{3/2}$ orbital to the $5d_{3/2}$ and $5d_{5/2}$ ones: a large white line is observed on oxidized platinum due to electron vacancy in the d-orbital, while the white line is small on reduced platinum due to the lack of an electron vacancy.[34] Thus, the electronic state of the Pt catalysts after the H_2-SCR was estimated by the integrated intensity of the white line in the Pt L_{III}-egde XANES spectra obtained by a curve-fitting analysis. First, we carried out the curve-fitting analysis with an arctangent and a Gaussian function,[35−37] but it was difficult to fit the spectra of Pt foil in our present study. To improve the curve-fitting analysis, we analyzed the spectra with a mixed Gaussian−Lorentzian function instead of the Gaussian function, as Kato et al. proposed in the Al K-edge XANES study.[38] The integrated white line intensities thus estimated are shown in Table 3. The order in the integrated white line intensity was Pt/MgO > Pt/Al_2O_3-60 > Pt/Al_2O_3-35 > Pt/BEA, Pt/Y, Pt/Al_2O_3-22 > Pt/MFI, Pt/SiO_2-Al_2O_3, Pt/MOR > Pt/SiO_2. This order indicates that the electron density in the 5d-orbital of the supported Pt is the lowest on Pt/MgO and the highest on Pt/ SiO_2. On the Pt catalysts supported on nonzeolitic metal oxides, this trend agreed well with the report by Yazawa et al.[37] In their report, they clearly correlated the integrated white line intensity with the acid−base property of the support material; platinum on the acidic support has a higher electron density in the 5d-orbital than that on a basic one, or, in other words, platinum on an acidic support is less oxidized than that on a basic one. It is expected that Yazawa's conclusion can be extended to the present results, although our present study includes Pt catalysts supported on zeolites.

Figure 4 shows the Fourier transforms of the Pt L_{III}-edge EXAFS spectra of supported platinum catalysts after the H_2-SCR and those of the Pt foil and PtO_2 as reference samples (the range of k is 4−15 $Å^{-1}$). The spectrum of Pt foil (spectrum a) showed a peak at $r = 2.65$ Å, which arises from the Pt−Pt shell (distance (R) = 2.77 Å, coordination number (N) = 12). The spectrum of PtO_2 (spectrum l) showed two peaks at R = 1.65 and 2.99 Å. The former at $R = 1.65$ Å arises from two kinds of Pt−O shells ($R = 1.988$ Å, $N = 4$, and $R = 2.004$ Å, $N = 8$), and the latter at $r = 2.99$ Å is from Pt−Pt shell (R = 3.136 Å, $N = 2$) and Pt−O shell ($R = 3.184$ Å, $N = 4$). All spectra of the supported platinum catalysts had a peak at R = 2.65 Å mainly due to the Pt−Pt shell in metallic platinum. As for the oscillations of Pt/Al_2O_3-60 and Pt/MgO, the peaks at R = 2.65 Å include a contribution of Pt−Al and Pt−Mg shell, respectively, derived from the mixed oxide of Pt and the support materials.[37] Pt/BEA (spectrum f), Pt/Y (spectrum g), Pt/Al_2O_3 (spectra h−j), and Pt/MgO (spectrum k) showed an additional peak about $R = 1.65$ Å, indicating that there is a Pt−O shell derived from Pt oxides.

As shown in Figure 4, the order of the peak intensity at R = 2.65 Å mainly due to the Pt−Pt shell in metallic platinum was Pt/SiO_2 > Pt/MFI > Pt/SiO_2-Al_2O_3 > Pt/ MOR > Pt/BEA > Pt/Y > Pt/Al_2O_3 > Pt/MgO. On the contrary, the order of the peak intensity of the Pt−O shell at $R = 1.65$ Å showed the opposite trend: Pt/MgO > Pt/ Al_2O_3-60 > Pt/Al_2O_3-35 > Pt/ Al_2O_3-22, Pt/Y, Pt/BEA. The presence of Pt−Al and Pt−Mg shell in Pt/Al_2O_3-60 and Pt/MgO indicates that the supported Pt is also in the oxidized state on these catalysts. The EXAFS results indicate that the fraction of metallic platinum decreases in the order of Pt/SiO_2 > Pt/MFI > Pt/SiO_2-Al_2O_3 > Pt/MOR > Pt/BEA > Pt/Y > Pt/Al_2O_3 > Pt/MgO. This trend is consistent with the Pt L_{III}-edge XANES results that the electron density of the supported Pt is in the same order, indicating that platinum on an acidic support is less oxidized than that on a basic one.

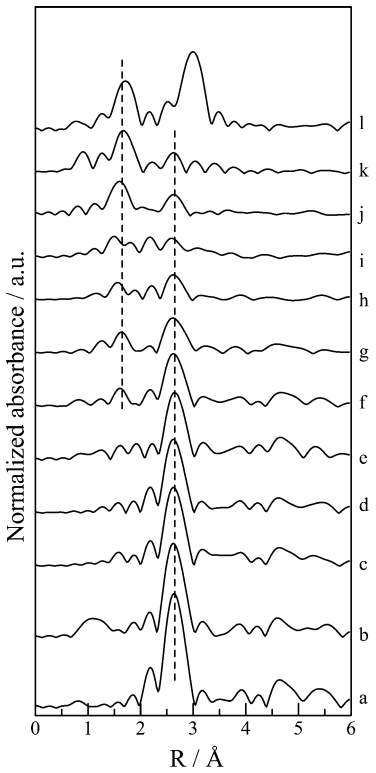

Figure 4. Fourier transforms of k^3-weighted Pt L_{III}-edge EXAFS spectra of (a) Pt foil, (b) Pt/SiO_2, (c) Pt/MFI, (d) Pt/SiO_2-Al_2O_3, (e) Pt/MOR, (f) Pt/BEA, (g) Pt/Y, (h) Pt/Al_2O_3-22, (i) Pt/Al_2O_3-35, (j) Pt/Al_2O_3-60, (k) Pt/MgO, and (l) PtO_2. The spectra of the catalysts (b−k) were measured after the H_2-SCR reaction.

3.4. In Situ IR. Figure 5 shows the in situ IR spectra of adsorbed species on various Pt catalysts under the H_2-SCR reaction conditions at 348 K. On Pt/MFI (Figure 5a), two strong bands at 1447 and 1626 cm^{-1} were mainly observed. The band at 1447 cm^{-1} is a typical absorption band of NH_4^+ ion adsorbed on Brønsted acid sites.[39−41] Actually, we confirmed the formation of the band at 1447 cm^{-1} by the introduction of NH_3 on the MFI support. Since the latter band was also observed in flowing $H_2 + O_2$ at 348 K, the band at 1626 cm^{-1} can be assigned to adsorbed water.[41] Although another possible assignment of the band at 1626 cm^{-1} is coordinately held NH_3 on Lewis acid sites,[41,42] the possibility of this assignment is very low for zeolite-based catalysts due to the presence of water vapor, which is produced by H_2 oxidation with NO and O_2, under the reaction conditions. In addition, four weak bands were observed at 1844, 1941, 2210, and 2235 cm^{-1}. The bands at 2210 and 2235 cm^{-1} are assigned to gas-phase N_2O.[43] The broad bands at 1844 and 1941 cm^{-1} can be assigned to NO species adsorbed on Pt.[41,44]

The bands due to NH_4^+ ion (1447 cm^{-1}), adsorbed H_2O (1626 cm^{-1}), and gas-phase N_2O (2210 and 2235 cm^{-1}) were also observed on the other Pt/zeolites and Pt/SiO_2-Al_2O_3 (Figure 5b−d). The band intensity of the NH_4^+ ion was the largest on Pt/MFI. On Pt/Al_2O_3-35, overlapping broad bands of some

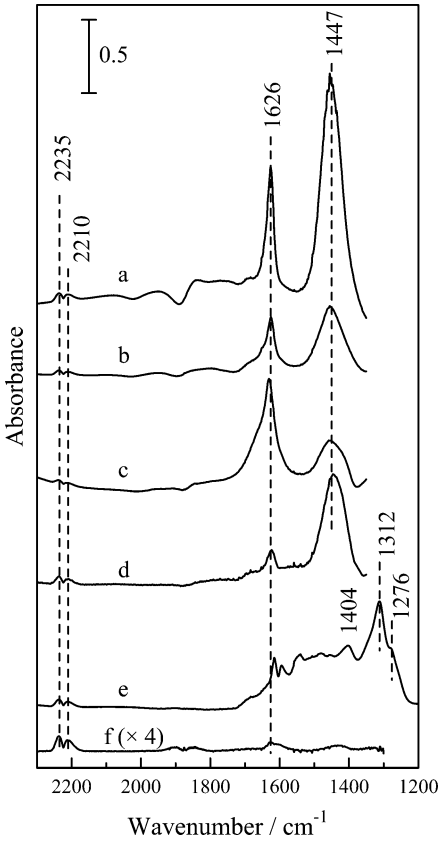

Figure 5. In situ IR spectra of adsorbed species on (a) Pt/MFI, (b) Pt/BEA, (c) Pt/Y, (d) Pt/SiO_2-Al_2O_3, (e) Pt/Al_2O_3-35, and (f) Pt/SiO_2 in flowing NO + O_2 + H_2 for 1 h at 348 K.

adspecies were observed in the range of 1200−1700 cm^{-1}. In these overlapping bands, a band at 1404 cm^{-1} and two bands at 1276 and 1312 cm^{-1} were assigned to the NH_4^+ ion on Al_2O_3[39] and surface nitrates,[45,46] respectively. Although the assignment of the other overlapping bands was difficult, these bands could be attributed to various adsorbed NO_x species such as NO_2, nitrate, and nitrite. On Pt/SiO_2, only small bands attributable to adsorbed H_2O and gas-phase N_2O were observed.

The reactivity of adsorbed species on Pt/MFI in flowing NO and O_2 was examined by the transient response of the IR spectra at 348 K. The catalyst was first exposed to flowing NO + O_2 + H_2 for 1 h. The catalyst was then exposed to flowing NO + O_2, while recording the IR spectra as a function of time. Figure 6 shows the dynamic change in the in situ IR spectra under flowing NO + O_2. Upon switching the flow to NO + O_2, the bands due to the gas-phase N_2O (2210 and 2236 cm^{-1}) immediately disappeared. The bands of the NH_4^+ ion (1454 cm^{-1}), adsorbed H_2O (1625 cm^{-1}), and adsorbed NO (1844 and 1941 cm^{-1}) gradually decreased with time on stream. The band of NH_4^+ disappeared after 60 min. New bands, which may be assigned to physisorbed NO_2,[41,47] appeared at 1347 and 1605 cm^{-1} after 30 min.

3.5. Reactivity of Adsorbed NH_3 Specices on Catalysts. The reactivity of adsorbed NH_3 species with NO and O_2 was confirmed at 348 K in the following manner. The catalysts were first exposed to a flow of 1000 ppm NH_3 for 1 h, followed by He purging for 10 min to remove the gas-phase NH_3 and weakly adsorbed NH_3 species. The catalysts were then exposed to flowing NO + O_2, and the gas-phase products were analyzed by gas chromatography after 30 min. Table 4 shows the N_2 and N_2O yields on supported Pt catalysts and on pure supports for this experiment. On Pt/MFI, 27% N_2 and 2% N_2O were

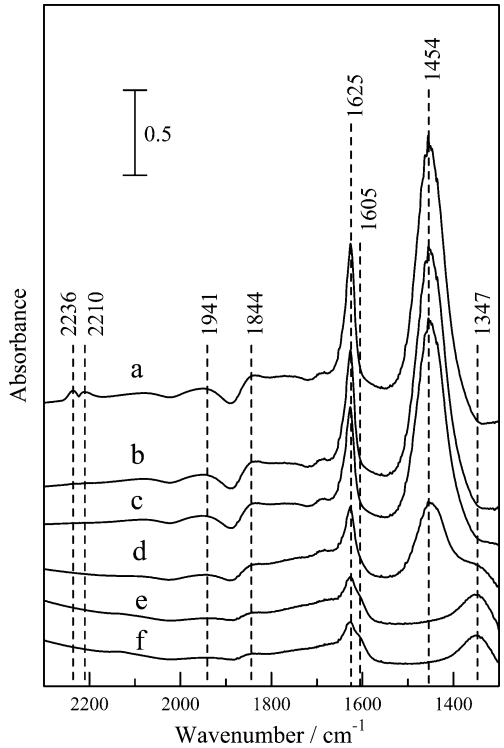

Figure 6. Dynamic changes in the in situ IR spectra as a function of time in flowing NO + O_2 on Pt/MFI at 348 K. The catalyst was preexposed to (a) a flow of NO + O_2 + H_2 for 1 h at 348 K and then in a flow of NO + O_2 for (b) 5 min, (c) 10 min, (d) 30 min, (e) 60 min, and (f) 120 min.

TABLE 4: N_2 and N_2O Yields after a Flow of NH_3 Followed by a Flow of NO + O_2 on Pt/Supports and Pure Supports. Reaction Temperature Was 348 K

	on Pt/support		on pure support	
support	N_2 yield/%	N_2O yield/%	N_2 yield/%	N_2O yield/%
Pt/MOR	A	*a*	36	0
Pt/MFI	27	2	44	0
Pt/BEA	*a*	*a*	36	0
Pt/Y	*a*	*a*	25	0
Pt/SiO_2-Al_2O_3	*a*	*a*	6	0
Pt/SiO_2	0	0	0	0
Pt/Al_2O_3-35	*a*	*a*	2	0

[a] Not measured.

produced, indicating that strongly adsorbed NH_3 species reacted with NO and O_2 to produce N_2 and a small amount of N_2O. On the other hand, neither N_2 nor N_2O was detected on Pt/SiO_2. Interestingly, the amount of N_2 produced on the pure MFI support was comparable to that on Pt/MFI. N_2O was not produced on the MFI support itself. A significant amount of N_2 was also produced on the other zeolite supports without the formation of N_2O. The N_2 yield on SiO_2-Al_2O_3 was much lower than those on zeolites but was higher than that on Al_2O_3. N_2 was not produced on SiO_2. The order of the N_2 yield on supports for this reaction test was MFI > BEA, MOR > Y > SiO_2-Al_2O_3 > Al_2O_3 > SiO_2, which agreed well with the order of the N_2 selectivity for the H_2-SCR on the supported Pt catalysts under steady-state conditions (Table 2).

The high reactivity of adsorbed NH_3 species is in a good agreement with the well-known NH_3-SCR activity of zeolites. Actually, Richter et al.[48,49] reported that NH_4^+ ions fixed on zeolites effectively reduces NO_x at low temperatures. The high storage capacity of NH_3 enhances the catalytic performance. Furthermore, they found that the NO_x conversion to N_2 is zero in the absence of oxygen, while the NO_x conversion increases

with the oxygen concentration. This is because the oxidation of NO to NO_2 by O_2 is a key step of the reaction. Actually, in our separate experiment, neither N_2 nor N_2O was produced over NH_3-adsorbed H-MFI at 373 K under flowing pure NO or pure O_2, while with flowing NO + O_2, the N_2 yield was 44% over the NH_3-adsorbed H-MFI. Therefore, NO_2, which is formed by the oxidation of NO by O_2, is indispensable to the conversion of adsorbed NH_3 to N_2.

The rate of NH_4^+ consumption was evaluated from the dynamic change in the band at 1454 cm^{-1} under flowing NO + O_2. By using the extinction coefficient of 0.147 cm^2 μmol^{-1} reported by Datka et al.,[50] the consumption rate of NH_4^+ on Pt/MFI was evaluated to be 122 ± 32 nmol g^{-1} s^{-1}, which was in a good agreement with the formation rate of N_2 (125 nmol g^{-1} s^{-1}) under the steady-state H_2-SCR reaction over Pt/MFI at 348 K. The agreement of these values means that the reaction between adsorbed NH_4^+ and NO + O_2 is the main pathway for the selective reduction of NO to N_2.

4. Discussion

4.1. Factor Controlling Activity of H_2-SCR. As for the selective catalytic reduction of NO by hydrogen (H_2-SCR), various types of catalysts have been reported, and their high performance is correlated to the important role of the noble metal and the reaction mechanism. During the initial step of the H_2-SCR on a Pt/SiO_2 catalyst, Burch et al. proposed the dissociation of NO into $N_{(ad)}$ and $O_{(ad)}$ followed by formation of N_2 and N_2O through the combination of the $N_{(ad)}$ species with each other or with another molecular NO species at high temperatures.[51] The activation of adsorbed NO followed by the reaction with $H_{(ad)}$[19,52] is also proposed, although this reaction pathway is an alternative interpretation to Burch's report, and the contribution of these reaction steps is still open to argument. Machida et al. related the high N_2 selectivity of Pt/TiO_2-ZrO_2 on the H_2-SCR to a stoichiometric reaction between H_2 and adsorbed nitrate.[22] Costas et al. proposed, based on an isotopic transient kinetic analysis, that both N_2O and N_2 are generated from the same active NO_x precursor (NO_2^+ and M−O−(NO)−O−M) in the H_2-SCR on Pt/La−Ce−Mn−O,[21] and the de-NO_x reaction must include a H-spillover process from Pt metal to the La−Ce−Mn−O support surface. Machicda et al. also clarified the importance of spillover in the H_2-SCR reaction over Pd/MnOx-CeO_2.[53] They found that the role played by Pd is to produce atomic hydrogen, which spills over onto the support and causes both the reduction of adsorbed nitrite and the reduction of the surface followed by a reaction between the anion vacancy and gaseous NO.

For the present study, these reaction steps should proceed on a platinum surface because the supports employed are practically inactive for these reactions below 400 K. It is expected that the H_2-SCR activity strongly depends on the property of the supported Pt species. For example, Machida et al. indicated that metallic Pt species shows a higher activity than the oxidized one by comparison of the H_2-SCR performance of oxidized and reduced Pt/TiO_2-ZrO_2 catalysts.[22] On the other hand, it is reported that the NO-H_2 reaction in the absence of O_2 on Pt/Al_2O_3 is structure-sensitive,[54] but information about the oxidation state of Pt is not obtained in these reports. Although the catalytic performance of the H_2-SCR on supported Pt catalyst should be dependent on the nature of the Pt species, these previous papers did not systematically discuss the effects of the individual properties of the Pt species, such as the dispersion and oxidation state of Pt. In this section, the relation between the property of the supported Pt species and the SCR activity is discussed.

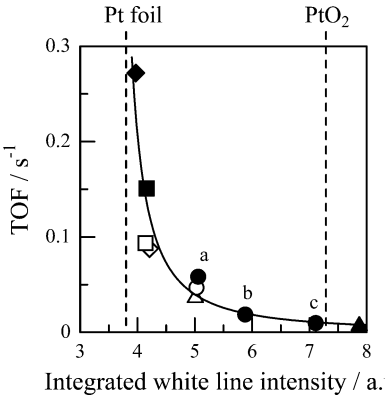

Figure 7. NO TOF over Pt catalysts, as a function of white line area intensity estimated from Pt L_{III}-edge XANES. Catalysts: (◇) Pt/MOR, (□) Pt/MFI, (△) Pt/BEA, (○) Pt/Y, (■) Pt/SiO_2-Al_2O_3, (◆) Pt/SiO_2, (●) Pt/Al_2O_3, and (▲) Pt/MgO. Symbols of a−c denote Pt/Al_2O_3-22, -35, and -60, respectively.

Figure 7 shows the relationship between the integrated white line intensity and turnover frequency for NO_x (TOF), estimated from the NO_x conversion and Pt dispersion. Irrespective of the support materials or Pt dispersion, the TOF increased with a decrease in the integrated white line intensity. Therefore, the figure clearly shows that metallic Pt species is a highly active species (i.e., the oxidation state of Pt is the controlling factor for the H_2-SCR activity). On the other hand, a significant difference in the TOF was observed in Pt/MOR, Pt/SiO_2-Al_2O_3, and Pt/Al_2O_3-22, although Pt dispersions measured after the reaction are in a very narrow range (Table 3). The results suggest that the geometry and ensemble size of Pt particles would be less effective for the H_2-SCR activity.

As shown in Table 3, Pt is more metallic when it is supported on a more acidic support. For instance, Pt/MFI is more metallic than Pt/Al_2O_3-22, although Pt dispersions are very close to each other, indicating a strong support effect on the oxidation state of the Pt species. Moreover, the EXAFS data suggested the formation of mixed oxides of Pt with supports in Pt/Al_2O_3-60 and Pt/MgO (Figure 4). Since the support effect is expected to be due to a certain electronic interaction between the noble metal and support material, it should be more appropriate to discuss the interaction in terms of the electronegativity of the support materials rather than the acidity. Yazawa et al. presented a clear relationship between the catalytic activity for propane combustion and the oxidation state of Pt on various supports, which was rationalized by the electrophilic/electrophobic property of the supports (i.e., higher electrophilic property provides less oxidized Pt resulting in the high catalytic activity).[34,37,55−56] The electrophobic (i.e., electron-donating) materials promote the noble metal oxidation since the noble metal oxo-anion such as $PtO_\alpha^{\delta-}$ is more stabilized on electron-donating support materials, such as MgO. Actually, on the basis of thermochemical data, the Pt compound with the alkaline earth group, $MPtO_\alpha$, shows a higher decomposition temperature than PtO_2, indicating that the alkaline earth metal stabilizes the $MPtO_\alpha$ binary oxide. For the supported Pt catalysts employed in this study, including the zeolite supports, the oxidation state of Pt under the H_2-SCR should also be controlled by the electron-withdrawing/electron-donating property of the supports.

4.2. Factor Controlling N_2 Selectivity of H_2-SCR. As shown in Figure 2, the behavior of the N_2 selectivity was dependent on the NO_x conversion. At higher conversions, the consecutive production of N_2 from N_2O was suggested as reported by Burch et al.[51] in the H_2-SCR on Pt/SiO_2. On the other hand, in the range of NO_x conversions below 60%, the N_2 selectivity was

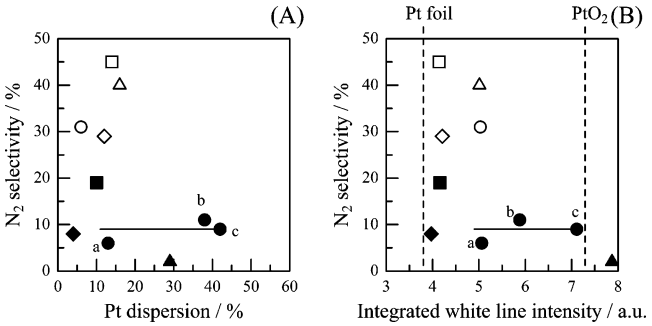

Figure 8. Dependence of N_2 selectivity at 348 K on (A) Pt dispersion and (B) white line area intensity estimated from Pt L_{III}-edge XANES of Pt catalysts. Catalysts: (◇) Pt/MOR, (□) Pt/MFI, (△) Pt/BEA, (○) Pt/Y, (■) Pt/SiO_2-Al_2O_3, (◆) Pt/SiO_2, (●) Pt/Al_2O_3, and (▲) Pt/MgO. Symbols of a−c denote Pt/Al_2O_3-22, -35, and -60, respectively.

almost independent of the NO_x conversion. Thus, at a lower NO_x conversion, the main route for the N_2 production is not the consecutive reaction of N_2O to N_2 but the direct N_2 production route from NO in the main route. This section focused on the effect of the supports on the N_2 selectivity during the initial reaction step of the H_2-SCR, based on the reaction data at a low NO_x conversion.

First, the influence of the properties of the Pt species on the N_2 selectivity is discussed. Figure 8A,B shows the N_2 selectivity as a function of the Pt dispersion and of the integrated white line intensity of all Pt catalysts after the H_2-SCR, respectively. The N_2 selectivity was correlated with neither the Pt dispersion nor the integrated white line intensity. Although Pt/MOR, Pt/MFI, and Pt/SiO_2-Al_2O_3 had comparable Pt dispersions and the same white line intensity, the N_2 selectivity significantly differed. Therefore, there is little contribution of the Pt properties for the N_2 selectivity. As a typical example, the N_2 selectivity was almost constant among the three Pt/Al_2O_3 catalysts with different dispersions and oxidation states of Pt.

Second, the relationship between the property of the support and N_2 selectivity is discussed. As shown in Table 2, the N_2 selectivities on Pt/zeolites were higher than those on Pt/metal-oxides and were in the order of Pt/MFI > Pt/BEA > Pt/Y, Pt/MOR. Pt/SiO_2-Al_2O_3 exhibited a high N_2 selectivity (19%) among the Pt/metal-oxides. Since zeolites and SiO_2-Al_2O_3 are typical strong solid acid catalysts, contribution of acid sites of the supports is suggested. Actually, the N_2 selectivity was correlated to the acid strength of the supports as follows. Katada et al. reported that the heat of adsorption of ammonia, which is a general measure of the acid strength of zeolites, is 145, 130, 120, and 110 kJ mol^{-1} for H-MOR, H-MFI, H-BEA, and H-Y, respectively.[57−59] The N_2 selectivity increases with the increase in the acid strength of zeolites, except for Pt/MOR. Because of the wide range of distribution of the acid strength on nonzeolitic oxides, a comparison of the acid strength is more difficult. However, the maximum acid strength of SiO_2-Al_2O_3 measured by the titration method is $H_0 = -12 \sim -14$,[60] which is higher than Al_2O_3 ($H_0 = 3.3$), SiO_2 (chemically neutral), and MgO ($H_0 = 22.3$).[37,61] These results suggest that the acid strength of supports is an important factor controlling the N_2 selectivity for the H_2-SCR on Pt catalysts.

The involvement of the acid site of the supports was evaluated by in situ IR spectra. As shown in Figure 5, the formation of NH_4^+ ions on Brønsted acid sites was observed during the H_2-SCR. The band intensity was in the order of Pt/MFI > Pt/BEA > Pt/Y > Pt/SiO_2-Al_2O_3 > Pt/Al_2O_3 > Pt/SiO_2, which was the same order on the N_2 selectivity for the H_2-SCR. The only exception was Pt/MOR, which showed a stronger NH_4^+ band

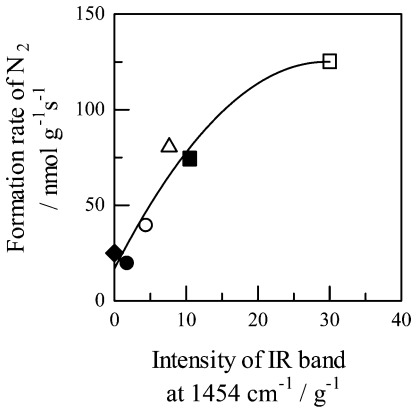

Figure 9. Rates of N_2 formation as a function of intensity of IR band at 1447 cm^{-1} (1404 cm^{-1} in Pt/Al_2O_3) in Figure 5. Catalysts: (□) Pt/MFI, (△) Pt/BEA, (○) Pt/Y, (■) Pt/SiO_2-Al_2O_3, (◆) Pt/SiO_2, and (●) Pt/Al_2O_3-35.

than Pt/MFI but lower N_2 selectivity. The lower N_2 selectivity on Pt/MOR may be rationalized by a strongly stabilized NH_4^+ ion on the strong acid sites of MOR. The contribution of NH_4^+ toward the overall reaction was confirmed in Figure 9(i.e., the rate of N_2 formation at 348 K was plotted vs the intensity of the band at 1454 cm^{-1} under the same reaction conditions). The Pt/MOR data were eliminated because of this reason. Clearly, the N_2 production rate increases with the increase in the band intensity due to the NH_4^+ ion at 1454 cm^{-1}, indicating that the formation of the NH_4^+ ion is a key for the selective production of N_2.

The reactivity of adsorbed NH_4^+ was verified by the reaction in a NO-containing atmosphere. As shown in Figure 6, the NH_4^+ ion was consumed in the flowing NO + O_2. Actually, N_2 was produced by the reaction of adsorbed NH_3 species, mainly NH_4^+ ion, on Pt/MFI and pure MFI itself in the flowing NO + O_2 (Table 4). The comparable N_2 yield on MFI to that on Pt/MFI in the $NH_{3(ad)}$−NO−O_2 reaction indicates that Pt is not essential for this reaction. The table indicates the following two facts: (1) NH_4^+ is a reactive species in flowing NO and O_2 and (2) Pt is not essential for the reaction of NH_4^+ and NO + O_2 (i.e., the support materials contribute to the selective formation of N_2). Furthermore, more directly, the agreement of the transient rate of NH_4^+ consumption and the steady-state formation rate of gaseous N_2 indicates that the reaction between adsorbed NH_4^+ and NO + O_2 is the main pathway for the selective reduction of NO to N_2, which can be expressed by the following equation:

$$4NH_4^+ + 4NO + O_2 \rightarrow 4N_2 + 6H_2O + 4H^+$$

Here, H^+ denotes the proton of the acidic hydroxyl group on the supports. Actually, the high reactivity of NH_4^+ ions on zeolites has been reported by Richter et al.[48] The N_2 yield in the transient reaction of adsorbed NH_3 species (Table 4) was higher on the supports having a higher acid strength, such as zeolites. The role of the support should be the stabilization and storage of NH_4^+ species on Brønsted acid sites because the order of the N_2 selectivity was in the same order of the acid strength.

4.3. Bifunctional Reaction Mechanism on Pt and Supports. In the present study, the selective reaction pathway was proposed in the H_2-SCR over supported Pt catalysts. This reaction pathway includes the NH_3 formation through NO reduction by H_2 on the Pt surface, followed by the migration and storage of NH_4^+ on the Brønsted acid sites of the acidic supports, and the selective N_2 formation through the reaction between NH_4^+ and NO_2 by the well-established NH_3-SCR mechanism. This selec-

SCHEME 1: Proposed Mechanism of SCR by H_2 over Pt Catalysts

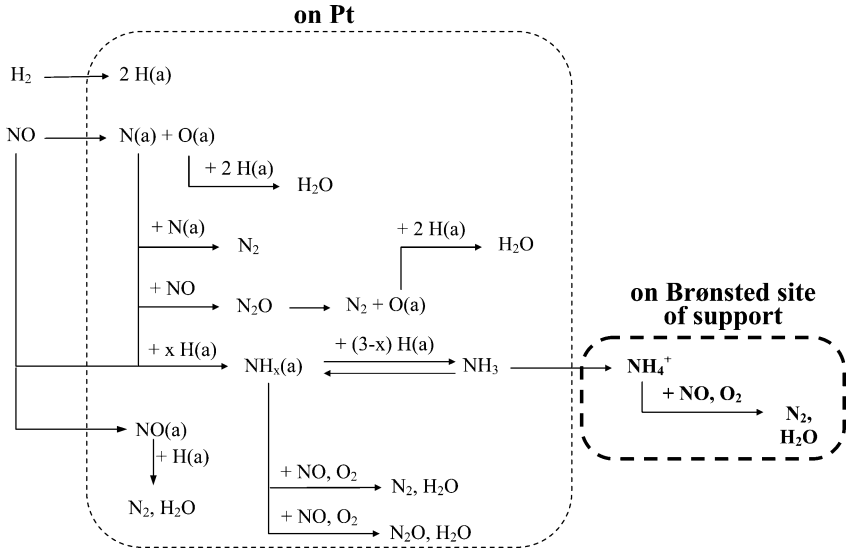

tive reaction was supported by the data shown in Figure 6 and Table 4. This route is a novel bifunctional route composed of NH_3 formation on the metallic platinum surface and the NH_4^+-SCR on the acidic supports.

Considering the other reaction pathways on the Pt surface, the reaction scheme on supported Pt catalysts can be proposed as shown in Scheme 1. As for the formation of NH_3, the reaction begins with the dissociation of H_2 into $H_{(ad)}$ and that of NO into $N_{(ad)}$ and $O_{(ad)}$ on the metallic platinum surface.[4,8] The $O_{(ad)}$ reacts with the $H_{(ad)}$ to produce H_2O. The $N_{(ad)}$ reacts with another $N_{(ad)}$ to form N_2, with NO to form N_2O, and with $H_{(ad)}$ to form $NH_{x(ad)}$. There is another reaction pathway for the production of N_2 over a platinum surface: the reaction between $NO_{(ad)}$ and $H_{(ad)}$. The existence of $NH_{x(ad)}$ is supported by the study of the NO + H_2 reaction over Pt(100) with HREELS and TPD.[62,63] By the consecutive reaction of $NH_{x(ad)}$ with $H_{(ad)}$, NH_3 should be formed. NH_3 or $NH_{x(ad)}$ species play the role of a reducing agent of NO; however, this reaction on the platinum surface leads to the production of both N_2 and N_2O, as confirmed by our data and the literature.[63] The migration of NH_3 from the platinum surface to the Brønsted acid sites of the support results in the formation and storage of NH_4^+. The Brønsted acid site of the supports provides a good reaction field for the selective reduction of NO_x by adsorbed NH_4^+ species.

5. Conclusions

The effect of supports on the H_2-SCR activity and N_2 selectivity of Pt catalysts was studied. The specific activity of Pt is controlled by the oxidation state of Pt (i.e., the more metallic Pt on the acidic supports shows a higher activity for the H_2-SCR). On the other hand, the selectivity is mainly controlled by the acid strength of the supports rather than the properties of Pt itself. More acidic supports provide a higher selectivity of N_2 formation on the Pt catalysts for the H_2-SCR. This is explained by a bifunctional mechanism composed of (1) the formation of the NH_4^+ intermediate on the metallic platinum surface through the NO reaction with H_2 and (2) the highly selective catalytic reduction of NO by ammonia on the acid sites of the supports that produces no N_2O. The advantage of the acidic support, such as zeolites, in the selective formation of N_2 is attributed to the storage capacity of the ammonia intermediate for the selective reaction pathway through NO and NH_4^+ on the acid sites.

Acknowledgment. The authors are grateful to Drs. Keiji Itabashi and Masao Nakano at Tosoh Co., Ltd., for providing the zeolite samples. This work was partly supported by a Grant-in-Aid from the Ministry of Education, Culture, Sports, Science and Technology, Japan. The X-ray absorption experiment was performed under the approval of the Photon Factory Program Advisory Committee (Proposal 2001G093).

References and Notes

(1) Iwamoto, M.; Yahiro, H.; Yu-u, Y.; Shundo, S.; Mizuno, N. *Shokubai (Catalyst)* **1990**, *32*, 430.
(2) Held, W.; Konig, A.; Richter, T.; Pupper, L. *SAE Pap*. **1990**, 900496.
(3) Hamada, H.; Kintaichi, Y.; Sasaki, M.; Ito, T. *Appl. Catal*. **1991**, *75*, L1.
(4) Burch, R.; Breen, J. P.; Meunier, F. C. *Appl. Catal. B* **2002**, *39*, 283.
(5) Konsolakis, M.; Macleod, N.; Issac, J.; Yentekakis, I. V.; Lambert, R. M. *J. Catal*. **2000**, *193*, 330.
(6) Denton, P.; Giroir-Fendler, A.; Praliaud, H.; Primet, M. *J. Catal*. **2000**, *189*, 410.
(7) Lee, J.-H.; Kung, H. H. *Catal. Lett*. **1998**, *51*, 1.
(8) Burch, R.; Millington, P. J. *Catal. Today* **1995**, *26*, 185.
(9) Burch, R.; Watling, T. C. *Appl. Catal. B* **1997**, *11*, 207.
(10) Traa, Y.; Burger, B.; Weitkamp, J. *Chem. Commun*. **1999**, 2187.
(11) Doumeki, R.; Hatano, M.; Kinoshita, H.; Yamashita, E.; Hirano, M.; Fukuoka, A.; Komiya, S. *Chem. Lett*. **1999**, 515.
(12) Seker, E.; Gulari, E. *J. Catal*. **1998**, *179*, 339.
(13) Giroir-Fendler, A.; Denton, P.; Boreave, A.; Praliaud, H.; Primet, M. *Top. Catal*. **2001**, *16/17*, 237.
(14) Ingelsten, H. H.; Skoglundh, M.; Fridell, E. *Appl. Catal. B* **2003**, *41*, 287.
(15) Burch, R.; Fornasiero, P.; Southward, B. W. L. *J. Catal*. **1999**, *182*, 234.
(16) Yokota, K.; Fukui, M.; Tanaka, T. *Appl. Surf. Sci*. **1997**, *121/122*, 273.
(17) Frank, B.; Emig, G.; Renken, A. *Appl. Catal. B* **1998**, *19*, 45.
(18) Burch, R.; Shestov, A. A.; Sullivan, J. A. *J. Catal*. **1999**, *188*, 69.
(19) Costa, C. N.; Stathopoulos, V. N.; Belessi, V. C.; Efstathiou A. M. *J. Catal*. **2001**, *197*, 350.
(20) Costa, C. N.; Savva, P. G.; Andronikou, C.; Lambrou, P. S.; Polychronopoulou, K.; Belessi, V. C.; Stathopoulos, V. N.; Pomonis, P. J.; Efstathiou A. M. *J. Catal*. **2002**, *209*, 456.
(21) Costa, C. N.; Efstathiou A. M. *J. Phys. Chem. B* **2004**, *108*, 2620.
(22) Machida, M.; Ikeda, S.; Kurogi, D.; Kijima, T. *Appl. Catal. B* **2001**, *35*, 107.
(23) Satsuma, A.; Hashimoto, M.; Shibata, J.; Yoshida, H.; Hattori, T.; *Chem. Commun*. **2003**, 1698.
(24) Breen, J. P.; Burch, R.; Lingaiah, L. *Catal. Lett*. **2002**, *79*, 171.
(25) Burch, R.; Coleman, M. D. *J. Catal*. **2002**, *208*, 435.
(26) Wisniewski, M.; Zawadzki, J. *Catal. Lett*. **2003**, *85*, 189.
(27) Nanba, T.; Kohno, C.; Masukawa, S.; Uchisawa, J.; Nakayama, N.; Obuchi, A. *Appl. Catal. B* **2003**, *46*, 353.

(28) Hattori, T.; Matsumoto, H.; Murakami, Y. *Stud. Surf. Sci. Catal.* **1987**, *31*, 815.
(29) Uchijima, T. *Catalytic Science and Technology*; Kodansha, Tokyo, 1990; Vol. 1, p 393.
(30) Komai, S.; Hattori, T.; Murakami, Y. *J. Catal.* **1989**, *120*, 370.
(31) Nomura, N.; Koyama, A. *KEK Rep. B* **1989**, *89*−*16*, 1.
(32) Satsuma, A.; Enjoji, T.; Shimizu, K.; Sato, K.; Yoshida, H.; Hattori, T. *J. Chem. Soc., Faraday Trans.* **1998**, *94*, 301.
(33) Satsuma, A.; Shimizu, K. *Prog. Energ. Combust.* **2003**, *29*, 71.
(34) Yoshida, H.; Yazawa, Y.; Hattori, T. *Catal. Today* **2003**, *87*, 19.
(35) Yoshida, S.; Tanaka. T. *X-ray Absorption Fine Structure for Catalysts and Surface (World Scientific Series on Synchrotron Radiation Techniques and Applications*; Iwasawa, Y., Ed.; World Scientific: Singapore, 1998; Vol. 2, p. 308.
(36) Horsley, J. A. *J. Phys Chem.* **1982**, *76*, 1451.
(37) Yazawa, Y.; Takagi, N.; Yoshida, H.; Komai, S.; Satsuma, A.; Tanaka, T.; Yoshida, S.; Hattori, T. *Appl. Catal. A* **2002**, *233*, 103.
(38) Kato, Y.; Shimizu, K.; Matsushita, N.; Yoshida, H.; Yoshida, T.; Satsuma, A.; Hattori, T. *Phys. Chem. Chem. Phys.* **2001**, *3*, 125.
(39) Knözinger, H. *Adv. Catal.* **1976**, *25*, 184.
(40) Eng, J.; Bartholomew, C. H. *J. Catal.* **1997**, *171*, 27.
(41) Nakamoto, K. *Infrared and Raman Spectra of Inorganic and Coordination Compounds*, 4th ed.; Wiley: New York, 1986.
(42) Robb, G. A.; Zhang, W.; Smirniotis, P. G. *Micropor. Mesopor. Mater.* **1998**, *20*, 307.
(43) Captain, D. K.; Amiridis, M. D. *J. Catal.* **2000**, *194*, 222.
(44) Citra, A.; Andrews, L. *J. Phys. Chem. A* **2000**, *104*, 8160.
(45) Parkyns, N. D. *Proceedings of the 5th International Congress on Catalysis*; Miami Beach, FL, 1972; Vol. 1, p 255.
(46) Shibata, J.; Shimizu, K.; Satokawa, S.; Satsuma, A.; Hattori, T. *Phys. Chem. Chem. Phys.* **2002**, *5*, 2154.
(47) Raj, A.; Le, T. H. N.; Kaliaguine, S.; Auroux, A. *Appl. Catal. B* **1998**, *15*, 259.
(48) Richter, M.; Eckelt, R.; Parlitz, B.; Fricke, R. *Appl. Catal. B* **1998**, *15*, 129.
(49) Richter, M.; Berndt, H.; Eckelt, R.; Schneider, M.; Fricke, R. *Catal. Today* **1999**, *54*, 531.
(50) Datka, J.; Gil, B.; Kubcka, A., *Zeolites* **1995**, *15*, 501.
(51) Burch, R.; Shestov, A. A.; Sullivan, J. A. *J. Catal.* **1999**, *186*, 353.
(52) Hecker, W. C.; Bell, A. T. *J. Catal.* **1985**, *92*, 247.
(53) Machida, H.; Kurogi, D.; Kijima, T. *J. Phys. Chem. B* **2003**, *107*, 196.
(54) Otto, K.; Yao, H. C. *J. Catal.* **1980**, *66*, 229.
(55) Yazawa, Y.; Yoshida, H.; Hattori, T. *Appl. Catal. A* **2002**, *237*, 139.
(56) Yazawa, Y.; Yoshida, H.; Takagi, N.; Komai, S.; Satsuma, A.; Hattori, T. *J. Catal.* **1999**, *187*, 15.
(57) Katada, N.; Igi, H.; Kim, J.-H.; Niwa, M. *J. Phys. Chem. B* **1997**, *101*, 5969.
(58) Katada, N.; Iijima, S.; Igi, H.; Kim, J.-H.; Niwa, M. *Stud. Surf. Sci. Catal.* **1997**, *105*, 1227.
(59) Katada, N.; Kageyama, Y.; Niwa, M. *J. Phys. Chem. B* **2000**, *104*, 7561.
(60) Hashimoto, K.; Masuda, T.; Ueda, H.; Kitano, N. *Appl. Catal.* **1986**, *22*, 147.
(61) Tanabe, K.; Misono, M.; Ono, Y.; Hattori, H. *Stud. Surf. Sci. Catal.* **1989**, *51*, 21.
(62) Zemlyanov, D. Y.; Smirnov, M. Y.; Gorodetskii, V. V.; Block, J. H. *Surf. Sci.* **1995**, *329*, 61.
(63) Smirnov, M. Y.; Zemlyanov, D. Y. *J. Phys. Chem. B* **2000**, *104*, 4661.